Int. J. Heat Mass Transfer. Vol. 21, pp. 1309–1324

0017-9310/78/1001-1309 $02.00/0

LAMINAR CONDENSATION HEAT AND MASS TRANSFER IN THE VICINITY OF THE FORWARD STAGNATION POINT OF A SPHERICAL DROPLET TRANSLATING IN A TERNARY MIXTURE: NUMERICAL AND ASYMPTOTIC SOLUTIONS

J. N. CHUNG* and P. S. AYYASWAMY†
University of Pennsylvania, Philadelphia, PA 19104, U.S.A.

(*Received* 3 *October* 1977 *and in revised form* 8 *March* 1978)

Abstract—Numerical solutions to the nonlinear, coupled boundary-layer equations governing laminar condensation heat and mass transfer in the vicinity of the forward stagnation point of a spherical droplet translating in a saturated mixture of three components are presented. The environment surrounding the droplet is composed of a condensable (steam), a noncondensable and nonabsorbable (air), and a third component which is noncondensable but absorbable (a typical fission product in a nuclear reactor containment following a loss of coolant accident). The investigation includes the range: droplet radius (0.005–0.05 cm), ambient thermal condition (75–175°C), initial temperature of droplet (5–170°C) and noncondensable and nonabsorbable component mass fraction in the bulk (0.01–0.5). The third component is taken to be in trace amounts. Asymptotic solutions that provide bounds and checks for the fully numerical solutions have also been included. The study exhibits several interesting features. A novel feature is that, for a given thermal driving force and noncondensable gas concentration in the bulk, the dimensionless heat transfer decreases with increasing ambient saturation temperature. An important conclusion arising out of the work is that, for laminar film condensation on a freely falling droplet, the droplet size, the forced flow field velocity and the ambient thermodynamic conditions prevailing in the environment are all strongly influencing and mutually related factors that control the transfer rates. The present results show good comparison with the existing, limited experimental results.

NOMENCLATURE

C_p, specific heat at constant pressure;
d_{eq}, equivalent diameter;
D, diameter;
$\mathscr{D}_{12}$, binary diffusion coefficient;
D_{ij}, multicomponent diffusion coefficients;
f, dimensionless stream function;
Fr, Froude number $= (4/9)(gR/U_\infty^2)$;
g, acceleration due to gravity;
h, heat-transfer coefficient for the Nusselt-type problem;
k, thermal conductivity of mixture;
$\dot{m}$, mass flux;
M, molecular weight;
p, pressure;
Pe, Peclet number $= 2U_\infty R/\kappa$;
Pr, Prandtl number $= \nu/\kappa$;
Q, heat flux;
r, radial distance from the axis of symmetry, r-direction in spherical coordinate;
R, radius of droplet;
Re, Reynolds number $= (3/2)(U_\infty R/\nu_\infty)$;
Sc, Schmidt number $= \nu/\mathscr{D}_{12}$;
Sc_{ij}, Schmidt number $= \nu/D_{ij}$;
t, time;
T, temperature;
T_0, instantaneous bulk temperature of droplet;
u, velocity in the x direction;
v, velocity in the y direction;
U_∞, terminal velocity of the droplet, free stream velocity;
w, mass fraction;
We, Weber number $= \rho d_{eq} U_\infty^2/\sigma$;
x, coordinate measuring distance along circumference from the stagnation point, mole fraction;
y, coordinate measuring radial distance outward from surface.

Greek symbols

δ, liquid film thickness in the Nusselt-type problem;
ΔT, $T_\infty - T_0$;
ΔT_i, $T_\infty - T_i$;
ε, mass fraction of third component in the bulk;
η, similarity variable $= yc^{1/2}/R$, $yc_*^{1/4}/R$;
θ, angle in spherical coordinates;
Θ, dimensionless temperature $(T - T_i)/(T_\infty - T_i)$;
Θ_l, $(T_l - T_i)/(T_\infty - T_i)$;
κ, thermal diffusivity $= k/\rho C_p$;
λ, latent heat of vaporization;
μ, dynamic viscosity;

*Graduate Student, Department of Mechanical Engineering and Applied Mechanics.
†Assistant Professor, Department of Mechanical Engineering and Applied Mechanics.

μ^*, ratio of inside to outside fluid medium viscosities;
ν, kinematic viscosity $= \mu/\rho$;
π, pi = 3.14159;
ρ, density;
σ, surface tension coefficient;
ϕ_{C_p}, ratio (C_p/C_{p_∞});
ϕ_k, ratio (k/k_∞);
ϕ_μ, ratio (μ/μ_∞);
ϕ_ν, ratio $(2v_\infty/v_l)$;
ϕ_ρ, ratio (ρ/ρ_∞);
Ψ, stream function.

Subscripts

e, at the outside edge of the mixture boundary layer;
g, gas;
i, at the liquid–mixture interface;
l, liquid;
l, i, in the liquid at the interface;
0, bulk condition in droplet;
s, at the s-surface;
v, vapor (steam);
v, i, in the vapor at the interface;
vg, i, in the mixture at the interface;
1, air;
2, vapor or steam;
3, third component;
∞, in the bulk phase, far away from the droplet.

INTRODUCTION

AN UNDERSTANDING of the condensation heat- and mass-transfer mechanisms associated with a droplet translating in a mixture is necessary in a variety of industrial processes and applications. For example, a knowledge of such transport rates is essential to the optimal design of nuclear reactor containment spray that is an integral part of the emergency core-cooling system. Also, the study of transport processes, either condensation or evaporation, between a freely falling droplet and its surrounding environment has been of classical interest. Several authors [1–11] have studied a variety of situations involving the heat and mass transfer from spherical droplets at various values of the Reynolds and Peclet numbers. Some of these contributions have been discussed in greater detail in this text where appropriate.

There does not seem to exist any systematic theoretical study of the laminar condensation on a translating spherical droplet in the presence of forced flow, multicomponent noncondensables and taking into account property variations. A complete solution of this problem of condensation over the entire droplet surface is too complicated and would require extensive and difficult numerical computations. As a necessary first step towards such a complete solution, we present here results of a study related to the laminar condensation heat and mass transfer in the vicinity of the forward stagnation point of a translating droplet. The value of this study is enhanced when one recognizes that the stagnation point behavior is likely to be dominant in determining the overall condensation rate on a translating droplet. Particularly, in reactor containment spray, the majority of a droplet's lifetime and certainly that portion during which the greatest condensation rate occurs is likely to be spent in a relatively high Reynolds number region, i.e. $Re > 100$ with respect to the surrounding vapor gas phase. Such a condition suggests the existence of laminar boundary layers in the vicinity of the forward stagnation point. Since boundary-layer thickness and consequently the inverse of heat- and mass-transport rates, are not likely to increase by over a factor of two over the leading portion of a body [12] and separation phenomena over the trailing portion substantially reduce the transport rates, stagnation point heat- and mass-transfer studies will provide important information regarding the relevant transfer rates.

In certain specific applications, laminar condensation on translating droplets takes place from a mixture which contains not only noncondensable components but also other noncondensable but absorbable components. For example, following a loss of coolant accident in a nuclear reactor, the containment atmosphere is likely to have air and certain other noncondensable but absorbable fission products in addition to steam. The present study also accounts for the presence of such a noncondensable but absorbable gas component that is present in trace amounts.

In this study we approach the stagnation point problem through both analytical and numerical techniques.

ANALYSIS

There are two primary objectives in the development of the analytical model for this study: (i) extension of the traditional laminar film condensation analysis on a freely falling cold water droplet to predict the heat- and mass-transfer rates at the forward stagnation point; and, (ii) an understanding of the effect of forced laminar film condensation on the transport of a third gas component in the mixture that is noncondensable but absorbable.

Consider then, a spherical water droplet of uniform temperature T_0, with fully developed internal circulation, that is falling at its terminal velocity, U_∞, in a large content of quiescent steam-air-third component (henceforth called steam-multicomponent) mixture at T_∞ which is higher than T_0. The third component is in trace quantities, and while noncondensable is absorbable. The mass fractions of the noncondensable components in the bulk of the mixture are prescribed. The total pressure of the system is given by the sum of the partial pressures of the saturated steam and that of air. The analytical model of the system is developed in terms of a set of vapor-gases—liquid boundary layers that are separated by a very thin condensate liquid interface. A schematic representation of the physical model and the coordinate system are shown in Fig. 1. The basic components within the vapor-gases boundary layer are the condensing vapor (steam), noncon-

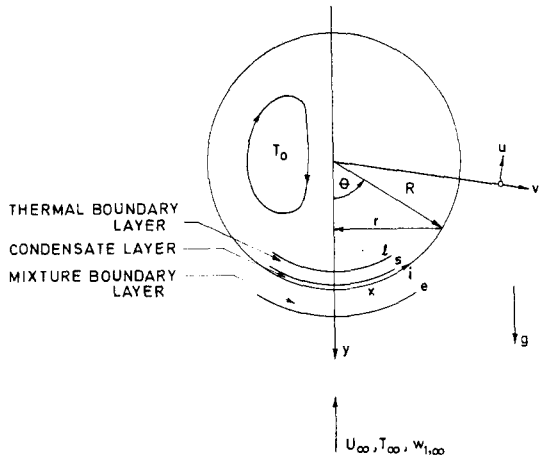

FIG. 1. Geometry and coordinate system.

densable and nonpermeable air and noncondensable but absorbable trace material, while in the liquid boundary layer, water is the only component. At the liquid and vapor-gases interface, the temperature T_i and mass fraction of air are generally unknown to begin with and are determined from certain compatibility conditions that are explained below. The solution is obtained by satisfying the conservation laws, the boundary conditions, and the compatibility conditions.

It is convenient to begin the analysis by separate considerations of each region in the model. We will also list the various assumptions made in the analysis where appropriate.

Region I: *liquid region*

(a) The thermal boundary layer within the droplet is assumed to be fully developed and thin. The fully developed assumption is justified when one considers the time required to attain a steady state. Levich *et al.* [7] and Ruckenstein [13] have shown that the time required to attain steady, thin, concentration boundary layers on a translating droplet is given by $(1+\mu^*)R/2U_\infty$, while Chao [10] has indicated that for $Pe > 500$, a criterion for the establishment time of a thin thermal boundary layer on a droplet is given by $U_\infty t/R = 1$. Therefore, the thermal boundary-layer growth is almost complete by the time the drop has moved a distance equal to its radius. (b) The liquid droplet is assumed to experience fully developed, vigorous internal circulation that is describable by the Hill's vortex solution. In many practical situations of interest, the droplet is introduced into the surrounding atmosphere by a spray nozzle. A strong internal circulation right after separation from such spray nozzles has been predicted by Sandry [14]. The internal circulation itself, in such cases, is likely to be induced due to the friction between the droplet outer surface and the nozzle internal wall. During the free fall, this internal circulation will be sustained because the retardation of the circulation due to the subsequent addition of liquid condensate is very minor. In fact, through an order of magnitude study, the inward velocity of the condensate, that would be expected to interfere with the internal circulation, can be shown to be an order of magnitude smaller than the axial surface velocity of the circulation. This feature can be appreciated when one considers the large difference in densities between the liquid and the condensing vapor. Thus, although there is a large heat flux, the accompanying mass flux is rather small, and most of this small condensate will be swept towards the rear stagnation point of the drop. Winnikow and Chao [9] with their experiments in highly purified systems have noticed that moving droplets invariably exhibit internal circulation. According to Chao [10], for droplet Reynolds numbers exceeding two hundred, the internal circulation flow field can be well described through an inviscid approximation. (c) The droplet will be assumed not to experience any oscillation. Winnikow and Chao [9] have observed in their experiments that droplets would experience little oscillation if the Weber number $We(=\rho d_{eq} U_\infty^2/\sigma)$ is less than 4. Our analysis will be restricted to this range. (d) Liquid properties inside the thermal boundary layer are taken to be constants. A simple 1/3 rule [15] will be used for establishing the reference temperature at which the liquid properties are to be evaluated. (e) The liquid droplet is assumed to remain spherical throughout the lifetime due to the effects of strong surface tension. Following the above assumptions, the internal circulation flow field and the governing equations appropriate to the liquid droplet are: for $r < R$,

$$v_l = \tfrac{3}{2}U_\infty\left(1-\frac{r^2}{R^2}\right)\cos\theta,$$

and,

$$u_l = -\tfrac{3}{2}U_\infty\left(1-2\frac{r^2}{R^2}\right)\sin\theta.$$

Applying the thin boundary-layer assumption, and letting $y = r-R$, $(|y|/R) \ll 1$, and noting that near the forward stagnation point, $\cos\theta \sim 1$ and $\sin\theta \sim 0$,

$$v_l \doteq -3U_\infty y/R, \quad u_l \doteq 0. \tag{1}$$

The energy equation for the thermal boundary layer in the liquid is reduced to the following:

$$-3U_\infty \frac{y}{R}\frac{\partial T_l}{\partial y} = \kappa_l \frac{\partial^2 T_l}{\partial y^2} \tag{2}$$

subject to:

$$\begin{aligned} T_l &= T_0 \quad \text{as} \quad y \to -\infty, \\ T_l &= T_s \quad \text{at} \quad s\text{-surface}. \end{aligned} \tag{3}$$

Region II: *thin interface of the condensate liquid*

In our analysis the axial velocity of the interfacial condensate layer is considered to vanish in the limit of approaching the stagnation point. Thus, for this layer, $u_{l,i} \to 0$ as $x \to 0$. It is important to note, however, that away from the stagnation point this liquid layer will move along with the axial surface velocity of the droplet surface and will be swept towards the rear stagnation point of the drop. At the outer boundary

(i-surface), this layer is assumed to have the inward radial velocity corresponding to the prevailing condensation rate. Furthermore, in view of the thinness of this layer, it will be assumed that the thermal resistance across this layer is negligibly small such that $T_s \doteq T_i$. The layer is thin owing to the sweeping motion which carries the condensate away towards the rear stagnation point. As we approach stagnation point, it is easy to see that the temperature gradient tends to zero in view of the thickness of the layer itself becoming vanishingly small.

Region III: *steam-multicomponent boundary layer*

(a) In view of the relatively high Reynolds number condition, $Re > 100$, that is likely to be present in the vicinity of the forward stagnation point, the flow field there will be taken to correspond to a laminar boundary layer. (b) Since the flow velocity range to be considered is moderate, viscous dissipation, compressibility effects and expansion work will be ignored. (c) The interfacial resistance, the thermal-diffusion and diffusion-thermo effects will be assumed to be negligible [16]. The steam multicomponent boundary-layer equations for ternary mixture are then as follows:

$$\frac{\partial}{\partial x}(\rho u r) + \frac{\partial}{\partial y}(\rho v r) = 0, \tag{4}$$

$$\rho u \frac{\partial u}{\partial x} + \rho v \frac{\partial u}{\partial y} = \frac{\partial}{\partial y}\left(\mu \frac{\partial u}{\partial y}\right) + \rho_\infty K^2 x + L(\rho - \rho_\infty), \tag{5}$$

$$\rho u \frac{\partial T}{\partial x} + \rho v \frac{\partial T}{\partial y} = \frac{1}{C_p}\frac{\partial}{\partial y}\left(k \frac{\partial T}{\partial y}\right) + \frac{\rho}{C_p}\left[(D_{11}C_{p_1} + D_{21}C_{p_2} + D_{31}C_{p_3})\frac{\partial w_1}{\partial y} + (D_{12}C_{p_1} + D_{22}C_{p_2} + D_{32}C_{p_3})\frac{\partial w_2}{\partial y}\right]\frac{\partial T}{\partial y}, \tag{6}$$

$$\rho u \frac{\partial w_1}{\partial x} + \rho v \frac{\partial w_1}{\partial y} = \frac{\partial}{\partial y}\left(\rho D_{11}\frac{\partial w_1}{\partial y}\right) + \frac{\partial}{\partial y}\left(\rho D_{12}\frac{\partial w_2}{\partial y}\right), \tag{7}$$

$$\rho u \frac{\partial w_2}{\partial x} + \rho v \frac{\partial w_2}{\partial y} = \frac{\partial}{\partial y}\left(\rho D_{21}\frac{\partial w_1}{\partial y}\right) + \frac{\partial}{\partial y}\left(\rho D_{22}\frac{\partial w_2}{\partial y}\right), \tag{8}$$

where

$$K = \frac{3}{2}\frac{U_\infty}{R} \quad \text{and,} \quad L = \frac{gx}{R}, \tag{9}$$

and subscripts 1, 2, and 3 refer to air, vapor, and third component, respectively. The expressions for the ternary diffusion coefficient which are highly sensitive to composition are given in [17]. The corresponding boundary conditions are:

$$e\text{-surface:} \quad u = (3/2)(U_\infty x/R), \quad T = T_\infty, \quad w_1 = w_{1,\infty}, \quad w_2 = w_{2,\infty}, \quad w_3 = \varepsilon, \tag{10}$$

and

$$i\text{-surface:} \quad T = T_i, \quad w_1 = w_{1,i}(T_i, p_\infty), \quad w_2 = w_{2,i}, \quad w_3 = 0, \quad u_{vg,i} = u_{l,i} \to 0. \tag{11}$$

Compatibility conditions:

(i) The interface is impermeable to air. Thus,

$$\left(\rho D_{11}\frac{\partial w_1}{\partial y} + \rho D_{12}\frac{\partial w_2}{\partial y} - \rho_1 v\right)_i = 0. \tag{12}$$

This condition is similar to Eckert–Schneider condition in mass-transfer cooling.

(ii) The energy balance equation which connects the two boundary layers is:

$$k_l \left.\frac{\partial T_l}{\partial y}\right|_{s\text{-surface}} = \dot{m}\lambda + k\left.\frac{\partial T}{\partial y}\right|_{i\text{-surface}}, \tag{13}$$

where,

$$\dot{m} = \text{mass condensation rate} = -\rho v|_{i\text{-surface}}. \tag{14}$$

Equation (2) subject to conditions (3) and equations (4)–(8) subject to surface conditions (10)–(14) must be solved.

SIMILARITY TRANSFORMATION

A similarity transformation can be effected through the use of:

$$\rho u = \frac{1}{r}\frac{\partial(\Psi r)}{\partial y}, \quad \rho v = -\frac{1}{r}\frac{\partial(\Psi r)}{\partial x}, \quad \eta = yC^{1/2}/R, \quad \Psi = \mu_\infty C^{1/2} x f/R, \quad \Theta = (T - T_i)/(T_\infty - T_i),$$

where

$$C = Re_\infty = \frac{3}{2}\frac{U_\infty R}{\nu_\infty}.$$

With the variables transformed as above, the similarity transformation yields the following ordinary differential equations for transport near the forward stagnation point:

$$\left[\phi_\mu\left(\frac{f'}{\phi_\rho}\right)'\right]' + 2f\left(\frac{f'}{\phi_\rho}\right)' + \left[1-\phi_\rho\left(\frac{f'}{\phi_\rho}\right)^2 + Fr(\phi_\rho - 1)\right] = 0, \tag{15}$$

$$\frac{1}{\phi_{C_p} Pr_\infty}[\phi_k \Theta']' + \frac{\phi_\mu}{C_p}\left(\frac{C_{p_1}}{Sc_{11}} + \frac{C_{p_2}}{Sc_{21}} + \frac{C_{p_3}}{Sc_{31}}\right) w_1' \Theta' + \frac{\phi_\mu}{C_p}\left(\frac{C_{p_1}}{Sc_{12}} + \frac{C_{p_2}}{Sc_{22}} + \frac{C_{p_3}}{Sc_{32}}\right) w_2' \Theta' + 2f\Theta' = 0, \tag{16}$$

$$\left(\frac{\phi_\mu w_1'}{Sc_{11}}\right)' + \left(\frac{\phi_\mu w_2'}{Sc_{12}}\right)' + 2f w_1' = 0, \tag{17}$$

$$\left(\frac{\phi_\mu w_1'}{Sc_{21}}\right)' + \left(\frac{\phi_\mu w_2'}{Sc_{22}}\right)' + 2f w_2' = 0, \tag{18}$$

and,

$$\Theta_l'' + \phi_\nu Pr_l \eta \Theta_l' = 0. \tag{19}$$

The boundary conditions are:

$$e\text{-surface:} \quad (f'/\phi_\rho) \to 1, \ \Theta \to 1, \ w_1 = 1 - w_{2,\infty} - w_{3,\infty}, \ w_2 = w_{2,\infty}, \ w_3 = w_{3,\infty} = \varepsilon, \text{ for } \eta \to \infty \tag{20}$$

$$i\text{-surface:} \quad \left(\frac{f'}{\phi_\rho}\right) = 0, \ w_2 = w_{2,i}(p_\infty, T_i), \ w_1 = 1 - w_{2,i}, \ \Theta_i = 0 = \Theta_{l,i}, \ \frac{\phi_\mu}{Sc_{11}} w_{1,i}' + \frac{\phi_\mu}{Sc_{12}} w_{2,i}' + 2f_i w_{1,i} = 0$$

where

$$f_i = \frac{\Delta T_i}{2 w_{2,i} \lambda}[k_l \Theta_{l,i}' - k\Theta_{vg,i}'] - \frac{\phi_\mu}{Sc_{21}} w_{1,i}' - \frac{\phi_\mu}{Sc_{22}} w_{2,i}' \tag{21}$$

$$l\text{-surface:} \quad \Theta_l = \Theta_{l,0} \quad \eta \to -\infty. \tag{22}$$

In equation (20) above, ε represents a trace quantity. $\Theta_{l,0}$ is the droplet inside bulk temperature.

SOLUTION PROCEDURE

Since the third component is in trace amounts, a regular perturbation analysis of the governing ordinary, nonlinear, differential equations (15)–(18) will be made in order to obtain a zeroth order and a first order set of equations. The resulting zeroth order equation will then correspond to the case of laminar condensation of binary mixture of vapor and noncondensable air on a translating droplet. The first order solution will describe the transport of the third component. Equation (19), in view of its simplicity, will be analytically solved. Consider writing,

$$\left.\begin{aligned} w_1 = w_{10} + \varepsilon w_{11} + \ldots, \ w_2 = w_{20} + \varepsilon w_{21} + \ldots, \ w_3 = \varepsilon w_{30} + \varepsilon^2 w_{31} + \ldots, \ f = f_0 + \varepsilon f_1 + \ldots, \\ \Theta = \Theta_0 + \varepsilon \Theta_1 + \ldots, \quad \text{and,} \quad \Theta_l = \Theta_{l0} + \varepsilon \Theta_{l1} + \ldots. \end{aligned}\right\} \tag{23}$$

Upon substitution of (23) in equations (15)–(18), the zeroth order equations are:

$$\left[\phi_\mu\left(\frac{f_0'}{\phi_\rho}\right)'\right]' + 2f_0[f_0'/\phi_\rho]' + \left[1 - \phi_\rho\left(\frac{f_0'}{\phi_\rho}\right)^2 + Fr(\phi_\rho - 1)\right] = O(\varepsilon), \tag{24}$$

$$\frac{1}{\phi_{C_p} Pr_\infty}(\phi_k \Theta_0')' + \frac{\phi_\mu}{Sc}\frac{C_{p_{1\to 2}}}{C_p} w_{10}' \Theta_0' + 2f_0 \Theta_0' = O(\varepsilon), \tag{25}$$

$$\left(\frac{\phi_\mu w_{10}'}{Sc}\right)' + 2f_0 w_{10}' = O(\varepsilon), \tag{26}$$

and

$$\Theta_l'' + \phi_\nu Pr_l \eta \Theta_l' = 0. \tag{27}$$

The corresponding boundary conditions and compatibility conditions become:

e-surface:

$$\frac{f_0'}{\phi_\rho} \to 1, \quad w_{20} = w_{2,\infty}, \quad w_{10} = 1 - w_{20}, \quad \Theta_0 = 1, \quad \eta \to \infty \tag{28}$$

i-surface:

$$\frac{f_0'}{\phi_\rho}=0,\quad \Theta_0=0,\quad w_{10}=1-w_{20},\quad w_{20}=w_{20}(p_\infty,T_i)=\frac{1-\dfrac{p_{v,i}(T_i)}{p_\infty}}{\left(\dfrac{M_v}{M_g}-1\right)\dfrac{p_{v,i}(T_i)}{p_\infty}+1},\quad \eta\to 0 \tag{29}$$

i-surface:

$$\frac{\phi_\mu}{Sc}w_{10}'+2f_{0,i}w_{10}=0,\quad f_{0,i}=\frac{\Delta T_i}{2\mu_\infty\lambda}(k_l\Theta_{l0,i}'-k\Theta_{vg0,i}'),\quad \eta\to 0 \tag{30}$$

l-surface:

$$\Theta_l=\Theta_{l,0},\quad \eta\to-\infty. \tag{31}$$

Next, the first order equations are:

$$\left[\phi_\mu\left(\frac{f_1}{\phi_\rho}\right)'\right]'+2f_0\left(\frac{f_1'}{\phi_\rho}\right)'+2f_1\left(\frac{f_0'}{\phi_\rho}\right)'-2\frac{f_0'f_1'}{\phi_\rho}=0, \tag{32}$$

$$\frac{1}{\phi_{c_p}Pr_\infty}(\phi_k\Theta_1')+\frac{\phi_\mu}{C_p}\left(\frac{C_{p_1}}{Sc_{11}}+\frac{C_{p_2}}{Sc_{21}}+\frac{C_{p_3}}{Sc_{31}}\right)(w_{10}'\Theta_1'+w_{11}'\Theta_0')$$
$$+\frac{\phi_\mu}{C_p}\left(\frac{C_{p_1}}{Sc_{12}}+\frac{C_{p_2}}{Sc_{22}}+\frac{C_{p_3}}{Sc_{32}}\right)(w_{20}'\Theta_1'+w_{21}'\Theta_0')+2(f_0\Theta_1'+f_1\Theta_0')=0, \tag{33}$$

and,

$$\left(\frac{\phi_\mu w_{11}'}{Sc_{11}}\right)'+\left(\frac{\phi_\mu w_{21}'}{Sc_{12}}\right)'+2(f_0w_{11}'+f_1w_{10}')=0, \tag{34}$$

$$\left(\frac{\phi_\mu w_{11}'}{Sc_{21}}\right)'+\left(\frac{\phi_\mu w_{21}'}{Sc_{22}}\right)'+2(f_0w_{21}'+f_1w_{20}')=0. \tag{35}$$

The corresponding boundary conditions and compatibility equations for the first order equations are:

e-surface:

$$\frac{f_1'}{\phi_\rho}\to 0,\quad \Theta_1=0,\quad w_{11}=-1,\quad w_{21}=0,\quad w_{30}=1,\quad \eta\to\infty \tag{36}$$

i-surface:

$$\left.\begin{aligned}&\frac{f_1'}{\phi_\rho}=0,\quad \Theta_1=0,\quad w_{11}=0,\quad w_{21}=0,\quad w_{30}=0,\\&\frac{\phi_\mu}{Sc_{11}}w_{11}'+\frac{\phi_\mu}{Sc_{12}}w_{21}'+2(f_0w_{11}+f_1w_{10})=0,\end{aligned}\right\}\quad \eta\to 0 \tag{37}$$

and

$$2(w_{20}f_1+w_{21}f_0)=\frac{\Delta T_i}{\mu_\infty\lambda}[k_l\Theta_{l1,i}'-k\Theta_{vg1,i}']-\frac{\phi_\mu}{Sc_{21}}w_{11}'-\frac{\phi_\mu}{Sc_{22}}w_{21}' \tag{38}$$

As expected, the above first-order equations reveal that the transport of the third component is dominantly controlled by the condensation process. It is also clear that the presence of the third component in trace amounts does not affect the main condensation flow.

The above set of equations (24)–(27) subject to conditions (28)–(31), and, equations (32)–(35) subject to conditions (36)–(38), were solved numerically by the "quasi-linearization" method. This method [18, 19] has been successfully used for two-point boundary value problems.

The calculation starts with an appropriate initial guess of the interface temperature $T_i(T_0<T_i<T_\infty)$, and then the simultaneous zeroth order equations are solved. With the zeroth order solutions as the input, the first order solutions are numerically evaluated by the same quasi-linearization technique. Now with the aid of the interface energy balance equations (30) and (38), the total interface flux $\Theta_{l,i}'$ is evaluated. Equation (19) for the thermal boundary layer in the liquid region is solved analytically to yield

$$\Theta_l=\Theta_{l,0}+\left(\frac{2}{\phi_v Pr_l}\right)^{1/2}\Theta_{l,i}'\int_0^\eta e^{-\zeta^2}\,d\zeta. \tag{39}$$

Therefore, the derived thermal boundary-layer edge temperature $\Theta_{l,0}$ is given by

$$\Theta_{l,0}=-\left(\frac{\pi}{2\phi_v Pr_l}\right)^{1/2}\Theta_{l,i}'. \tag{40}$$

Here for a guessed T_i, the vapor boundary-layer solutions as explained earlier provide $\Theta'_{i,i}$. Thus $\Theta_{l,0}$ can be evaluated using equation (40). The $\Theta_{l,0}$, however, corresponds to the initial temperature of the droplet when it is introduced into the mixture and is known *a priori*. The difference between the calculated $\Theta_{l,0}$ and the actual $\Theta_{l,0}$ serves to provide a convergence criterion. The criterion used in this study is:

$$|(\Theta_{l,0_{\text{calc.}}} - \Theta_{l,0_{\text{act.}}})/\Theta_{l,0_{\text{act.}}}| \lesssim 10^{-3}. \quad (41)$$

The entire calculation procedure is repeated until the desired convergence criterion is met.

An important observation is made at this stage with regard to the use of quasi-linearization methods. Faster convergence is attained with the method as long as the noncondensable air fraction is moderately high. With $w_{1,\infty} \to 0$, say, $w_{1,\infty} < 0.05$, condensation process is rather vigorous and the computations become expensive.

ASYMPTOTIC SOLUTION OF THE ZEROTH ORDER EQUATIONS WHEN $w_{1,\infty} \to 0$

We recall that the zeroth order solutions correspond to the case of laminar condensation of a binary mixture of vapor and a noncondensable on a translating droplet. As mentioned earlier, the numerical procedure becomes computationally expensive with $w_{1,\infty} \to 0$. However, with $w_{1,\infty} \to 0$, with properties evaluated at a reference temperature together with the neglect of buoyancy effects, it is possible to obtain an asymptotic solution to the zeroth order equations. This asymptotic solution provides trends that serve as checks for the results obtained from the numerical scheme.

With a procedure similar to that of Acrivos [20], the governing equations become:

$$f''' + 2ff'' + [1 - f'^2] = 0, \quad (42)$$

$$\psi'' + 2Scf\psi' = 0, \quad (43)$$

and

$$\frac{\Theta''}{Pr_\infty} + \frac{1}{Sc}\frac{C_{p_{1\to 2}}}{C_p}(w_{1,\infty} - w_{1,i})\psi'\Theta' + 2f\Theta' = 0, \quad (44)$$

where

$$\psi = (w_1 - w_{1,i})/(w_{1,\infty} - w_{1,i}). \quad (45)$$

The boundary conditions are:

$$f = \frac{n}{2Sc}\psi', \ \Theta = 0, \ \psi = 0, \ f' = 0, \ \eta = 0 \quad (46)$$

and

$$f' = 1, \ \psi = 1, \ \Theta = 1, \ \eta \to \infty \quad (47)$$

where, $n = (w_{2,\infty} - w_{2,i})/(1 - w_{2,i})$.

Introduce the interface flux b through:

$$\left.\frac{d\psi}{d\eta}\right|_{\eta=0} = b \text{ with } b \to \infty \text{ as } n \to 1, \quad (48)$$

and defining,

$$z = b\eta, \quad f = \frac{nb}{2Sc} + \frac{1}{b}\phi(z). \quad (49)$$

Noting that $\psi = \psi(z)$, $\Theta = \Theta(z)$, we get,

$$\phi''' + \frac{n}{Sc}\phi'' = \frac{1}{b^2}(\phi'^2 - 2\phi\phi'' - 1). \quad (50)$$

As $n \to 1$, then,

$$\phi''' + \frac{n}{Sc}\phi'' \doteq 0. \quad (51)$$

Also,

$$\psi'' + 2Sc\left(\frac{n}{2Sc} + \frac{\phi}{b^2}\right)\psi' = 0, \quad (52)$$

and,

$$\frac{\Theta''}{Pr_\infty} + \frac{1}{Sc}\frac{C_{p_{1\to 2}}}{C_p}(w_{1,\infty} - w_{1,i})\psi'\Theta' + 2\left(\frac{n}{2Sc} + \frac{\phi}{b^2}\right)\Theta' = 0. \quad (53)$$

The boundary conditions become:

$$\phi = 0, \ \phi' = 0, \ \psi = 0, \text{ and, } \Theta = 0 \text{ at } z = 0, \quad (54)$$

and

$$\phi' = 1, \ \psi = 1, \ \Theta = 1 \quad \text{as} \quad z \to \infty. \quad (55)$$

From equations (51) and (52), with $b \gg 1$, (see Appendix A),

$$b = \left(\frac{2Sc}{(1-n)(1+Sc)}\right)^{1/2}. \quad (56)$$

The condensate flux, $\dot{m}$, now becomes

$$\dot{m} = -\rho v|_{\eta=0} = \frac{\mu_\infty C^{1/2} n}{RSc}\left(\frac{2Sc}{(1-n)(1+Sc)}\right)^{1/2}. \quad (57)$$

Next, with $b \to \infty$ and $n \to 1$, it can be shown (see Appendix A), that the interface convective heat flux,

$$\Theta'_i = \frac{(1-\Theta_i)e^{\alpha}b}{I} \quad (58)$$

where,

$$I = \frac{1}{n}\sum_{j=0}^{\infty}\frac{A_1^j}{j!}\frac{1}{\left(\frac{A_2}{n} + j\right)},$$

$$\alpha = A_1 = \frac{Pr_\infty}{Sc}\frac{C_{p_{1\to 2}}}{C_p}(w_{1,\infty} - w_{1,i}),$$

and,

$$A_2 = Pr_\infty n/Sc.$$

For many practical situations, $A_1 < 1$, and the infinite series above converges rapidly. The total heat flux

$$Q = \dot{m}\lambda + k\left.\frac{\partial T}{\partial y}\right|_{i\text{-surface}} = \frac{C^{1/2}}{R}\left(\frac{\mu_\infty nb}{Sc} + \frac{k\Delta T_i(1-\Theta_i)e^{\alpha}b}{I}\right). \quad (59)$$

RESULTS AND DISCUSSION

Numerical and asymptotic solutions for condensation heat transfer to a translating droplet are

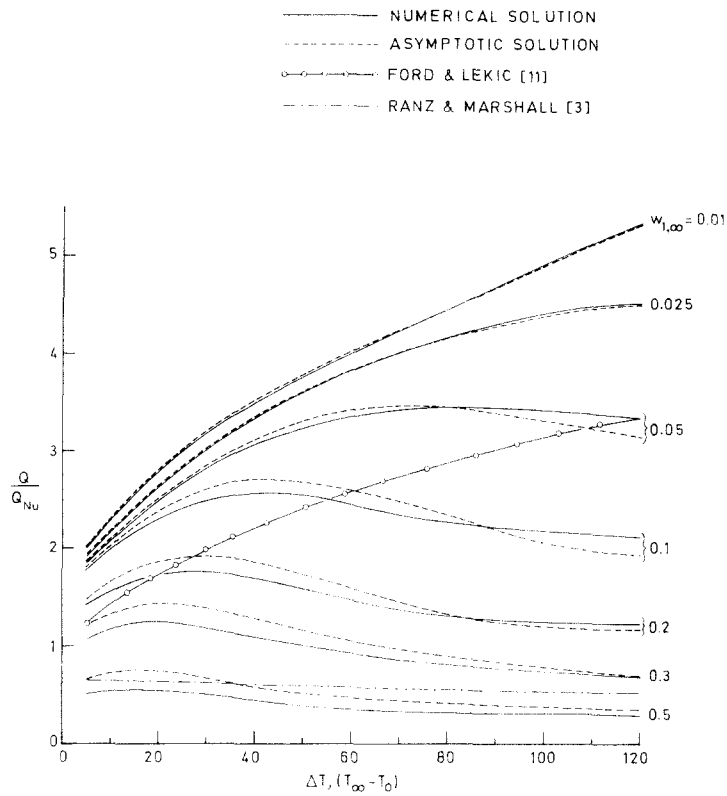

FIG. 2. Effect of $w_{1,\infty}$ on condensation heat transfer. $R = 0.025$ cm, $T_\infty = 125°C$, 146 cm/s $< U_\infty <$ 153 cm/s.

presented in the form of Q/Q_{Nu}, where Q_{Nu} is the heat flux corresponding to a Nusselt type condensation heat transfer near the upper stagnation point of an isothermal sphere situated in quiescent, pure, saturated steam. This manner of presentation of results explicitly exhibits the features introduced by the presence of noncondensables and forced flow for various drop bulk temperatures. The details for the derivation of Q_{Nu} itself are shown in Appendix B. The bulk medium is taken to be in saturated condition. Thus, the effects of superheating are not included, but these effects are known to be of minor importance [16].

The droplet sizes and the thermodynamic range chosen for the calculations are closely related to the operating conditions that are likely to prevail in the containment spray atmosphere of a nuclear reactor following a loss of coolant accident. The third component present in trace amounts may be taken to be the fission product elemental iodine [21]. Through such a choice the engineering value of this study becomes apparent.

Figures 2–5 show the effects of the presence of a noncondensable gas. In Fig. 2, the variation in the noncondensable gas mass fraction is in the wide range $0.01 < w_{1,\infty} < 0.5$. The curves give (Q/Q_{Nu}) as a function of $(T_\infty - T_0)$, for various $w_{1,\infty}$. The radius R of the droplet is 0.025 cm. The terminal velocities, U_∞, corresponding to various ambient conditions have been calculated using an equation recommended by Lapple [22]:

$$U_\infty = \frac{0.153 g^{0.714} D^{1.142} (\rho_L - \rho_\infty)^{0.714}}{\rho_\infty^{0.286} \mu_\infty^{0.428}}, \quad 2 \leqslant Re_\infty \leqslant 1000. \tag{60}$$

It is recognized that the terminal velocity given by equation (60) does not reflect the effects due either to the interfacial condensation velocity or the increase in droplet size. However, when we note that the interfacial velocity is small while the increase in droplet size is also negligibly small, then we can ignore these effects without introducing any appreciable errors. These U_∞ values vary in the neighborhood of 150 cm/s for the conditions chosen. The free stream bulk temperature is taken to be 125°C. For a given ΔT, (Q/Q_{Nu}) decreases with increasing $w_{1,\infty}$. The reason for the reduction in heat transfer due to the presence of the noncondensable is that in the steady state, the noncondensable gas will have a very steep concentration profile in the close vicinity of the interface. It is only with such a steep concentration gradient can the diffusive back flow balance the convective inflow. The build up of the noncondensable gas at the interface, however, causes a corresponding reduction in the partial pressure of the vapor at the interface. In turn, this reduces the saturation temperature at which the condensation takes place. The net effect is to lower the effective ΔT, thereby reducing the heat transfer [16]. The chain line in Fig. 2 corresponds to the Ranz and

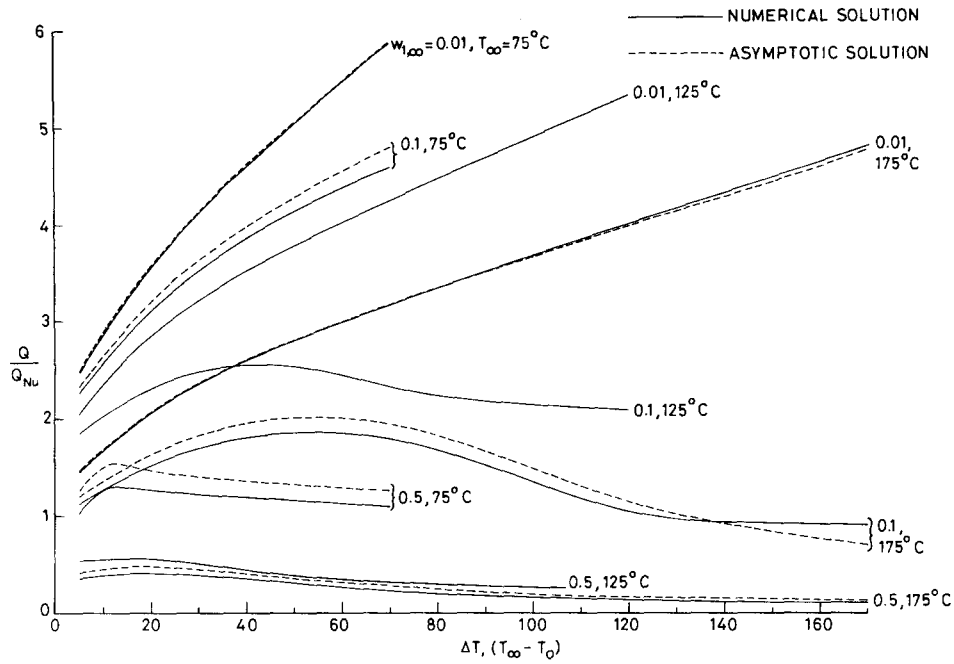

FIG. 3. Effects of T_∞ and $w_{1,\infty}$ on condensation heat transfer. $R = 0.025$ cm; $T_\infty = 175$°C, 107 cm/s $< U_\infty$ < 115 cm/s; $T_\infty = 125$°C, 146 cm/s $< U_\infty < 153$ cm/s; $T_\infty = 75$°C, 172 cm/s $< U_\infty < 175$ cm/s.

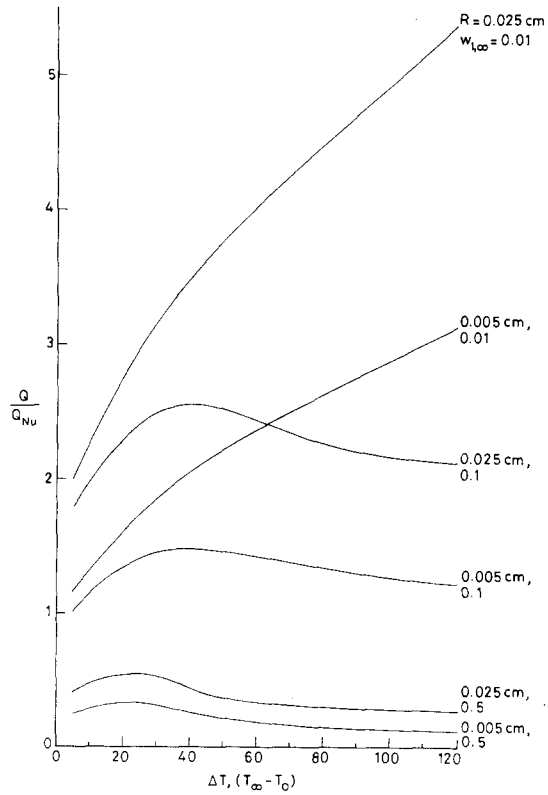

FIG. 4. Effects of droplet radius R and $w_{1,\infty}$ on condensation heat transfer. $T_\infty = 125$°C; $R = 0.025$ cm, 146 cm/s $< U_\infty$ < 153 cm/s; $R = 0.005$ cm, 23 cm/s $< U_\infty < 25$ cm/s.

Marshall correlation [3] that is used to describe the heat transfer from a droplet evaporating into a normal atmosphere. This correlation has been extensively used in nuclear industry to predict the heat and mass transfer to containment spray droplets. From the present investigation, it is seen that, for the ambient thermal conditions and droplet size used in Fig. 2, the correlation yields reasonable results only when about 30–50% of the containment atmosphere consists of the noncondensable gas. Otherwise, the use of the correlation could lead to appreciable errors.

Figure 2 also provides a comparison of the heat transfer results of this study with those of Ford and Lekic [11] obtained for a slightly different situation. This comparison is not obvious and needs a bit of explanation. The latter authors provide an approximate time-dependent correlation equation for the growth of water drops during condensation in direct contact with pure steam (no noncondensable present). Their correlation agrees well with their own experimental results for the growth. This growth equation is in a form that can be differentiated with respect to time and an equation describing the average heat transfer to the droplet can then be produced. The resulting equation will be time-dependent. By setting the time parameter value there equal to the time taken for the establishment of the thermal boundary layers in droplets studied in the present investigation, we are able to have a basis for directly comparing our quasi-steady results with their transient results. Since their correlation is for condensation from pure steam, we would expect reasonable agreement with our results in the limit of $w_{1,\infty} \to 0$. In particular, the comparison with the case where $w_{1,\infty}$ forms a mere 1% of the mixture could be appreciated. Their results are for droplets that are approximately three times bigger than those investigated in the present study, and furthermore, they correspond to average heat transfer,

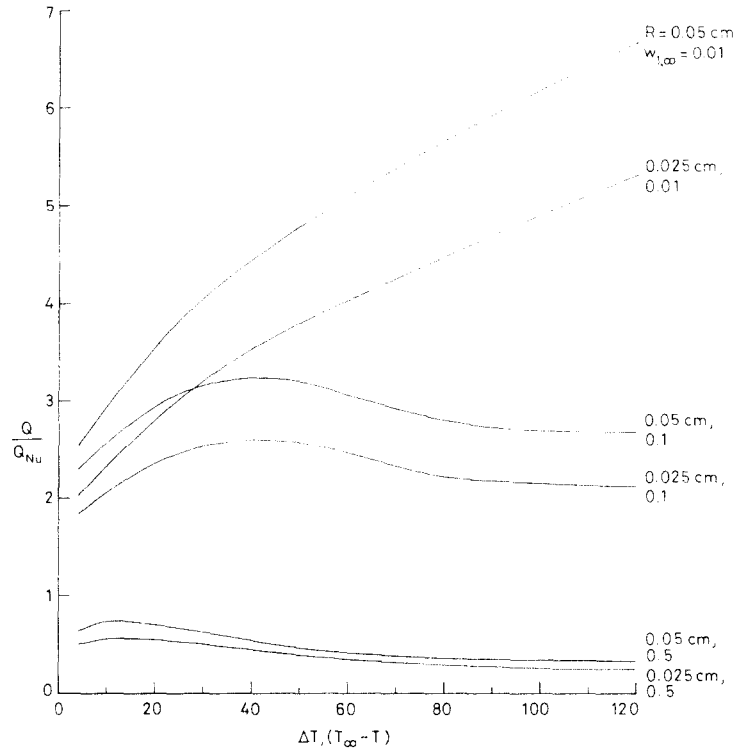

FIG. 5. Effects of droplet radius R and $w_{1,\infty}$ on condensation heat transfer. $T_\infty = 125°C$; $R = 0.05$ cm, 322 cm/s $< U_\infty <$ 335 cm/s; $R = 0.025$ cm, 146 cm/s $< U_\infty <$ 153 cm/s.

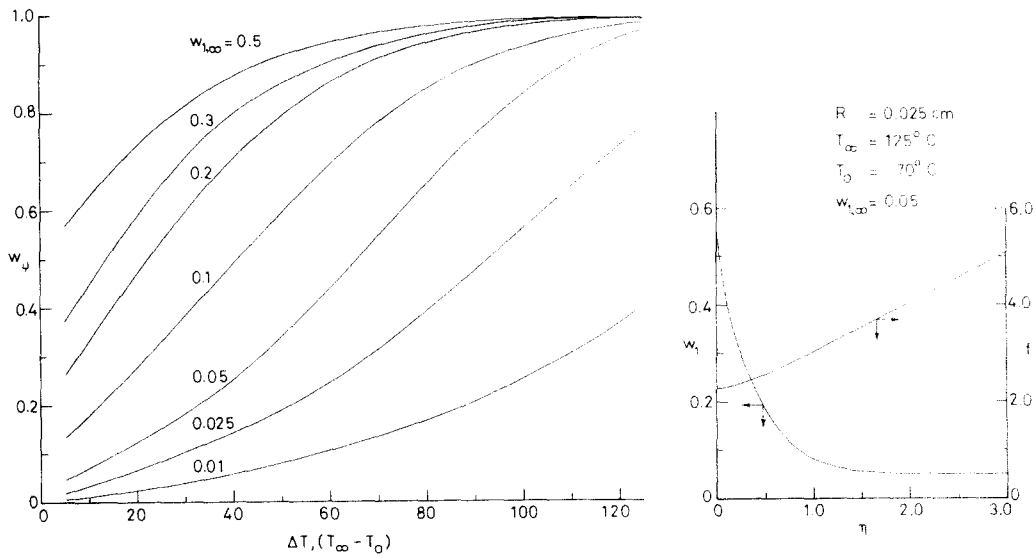

FIG. 6. The build-up of noncondensable air at the interface: a typical mass fraction distribution for air, and a typical inward velocity profile. $T_\infty = 125°C$; $R = 0.025$ cm.

while the present investigation provides stagnation point heat transfer. The stagnation point values will, of course, be higher. The graph shows that the present results are about 40% higher than those of Ford and Lekic, but in view of the above observations, it must be taken to represent reasonably good agreement. There is, in fact, no overwhelming reason why the comparison should be any better. More importantly, the trend is correct.

Figure 6 shows the variation in the steady state, interface mass fraction value of the noncondensable for various values of ΔT and $w_{1,\infty}$. The results are for a drop of 0.025 cm radius and a constant bulk temperature of 125°C. For a given bulk concentration, with increasing thermal driving force, the interface gas mass fraction increases steeply. This figure also shows a typical noncondensable gas concentration profile as a function of the distance from the interface. The profile

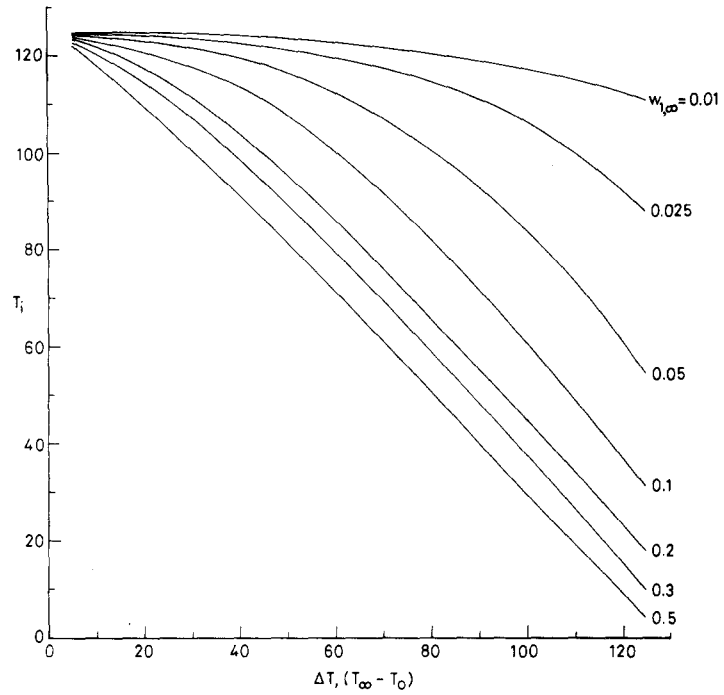

FIG. 7. The effect of $w_{1,\infty}$ on the temperature T_i. $T_\infty = 125°C$; $R = 0.025$ cm.

has a steep gradient in the close vicinity of the interface. Figure 7 is a plot of the interface temperature as a function of ΔT for various $w_{1,\infty}$. With increasing thermal driving force, the interface temperature decreases. This is because, with increasing ΔT, the noncondensable gas concentration at the interface increases with the result the saturation temperature is lowered there as previously explained. For a given ΔT, the interface temperature is higher for lower $w_{1,\infty}$.

Figure 3 shows the variation of (Q/Q_{Nu}) with ΔT for different $w_{1,\infty}$ and for selected ambient saturation temperatures. The objective is to ascertain the effect of the ambient saturation temperature (or pressure) on the heat transfer. The droplet size is 0.025 cm. Results appropriate to three different prescribed ambient temperatures are presented. For given ΔT and $w_{1,\infty}$, the dimensionless heat transfer decreases with increasing ambient saturation temperature. This is a new feature observed in the present study. In most cases usually studied, the film condensation, jointly with forced convection or not, occurs where the free stream flow field is independent of the prevailing ambient conditions. Then the dimensionless heat transfer has been noted to increase with increasing saturation temperature (pressure). In such cases the rate of condensation can be controlled by simply varying the ambient thermal conditions. For example, when one considers film condensation on a circular cylinder [23], it is observed that the heat transfer increases with increasing saturation temperature (pressure). However, in the case of condensation on a translating droplet, the free stream flow field cannot be independently manipulated and is intimately related to the prevailing ambient conditions. In particular, the flow field is seriously affected by the ambient temperature. With increased ambient temperature, for a given droplet size, the terminal velocity (or the free stream velocity) decreases. The condensation flow field is thus weakened and hence a decrease in dimensionless heat transfer is observed. Our results show that the weakening of the flow field due to reduced terminal velocity has a more serious effect on heat transfer than that of the increased ambient temperature (increased thermal driving force).

Figures 4 and 5 show the variations of (Q/Q_{Nu}) with ΔT for various droplet sizes and $w_{1,\infty}$. The ambient thermal condition is fixed at 125°C. The droplet sizes vary from 0.005 to 0.05 cm. For a given ΔT and $w_{1,\infty}$, the dimensionless heat transfer increases with increasing radius. It is evident from equation (60) that the terminal velocity of the droplet is a function of the droplet size as well. Hence, with increasing droplet size, the flow field is more vigorous. We can thus explain the increased heat transfer. In this same context, it can be shown from a simple nondimensional analysis that (Q/Q_{Nu}) for a translating droplet is proportional to $U_\infty^{1/2}/R^{1/4}$, where $U_\infty = U_\infty(R)$. The results presented in Figs. 4 and 5 qualitatively confirm such a dependence.

It is recalled that the total heat flux in our problem is made up of two parts: the heat transfer associated with a change of phase and the forced convective contribution. Figure 8 presents the ratio of the convective heat flux to the condensation heat flux as a function of ΔT for various $w_{1,\infty}$. We note that where large noncondensable gas concentrations and small thermal driving forces are encountered, the convective contribution may not be ignored for obtaining sufficiently

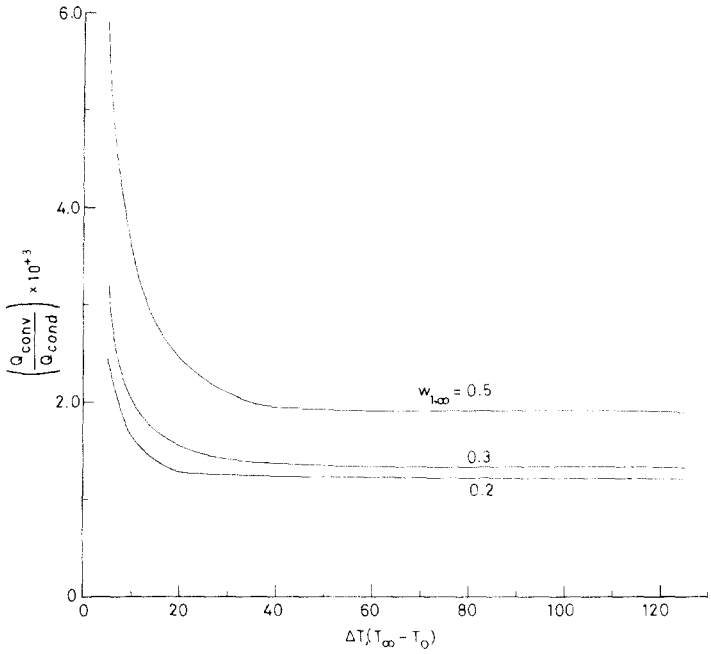

FIG. 8. Ratio of convective heat flux to condensation heat flux. $T_s = 125°C$; $R = 0.025$ cm.

accurate results. Outside these ranges, the heat transfer is almost entirely due to condensation.

Next, with $w_{1,\infty} \to 0$, we have obtained asymptotic solutions to the zeroth order equations. The results are shown by dotted lines in Figs. 2 and 3. The asymptotic solutions are in excellent agreement with the exact numerical solutions for $w_{1,\infty}$ less than 0.025. As expected, the deviation between the asymptotic and exact solutions grows with increasing $w_{1,\infty}$, and the asymptotic solutions introduce errors by as much as 50% when $w_{1,\infty}$ is about 0.5. For a certain range of ΔT and for a moderate $w_{1,\infty}$, the asymptotic solutions under-predict the heat transfer relative to the exact solution. This behavior is attributable to the constant property assumption adopted in the asymptotic method.

With decreasing $w_{1,\infty}$, the condensation becomes vigorous, and the computations become time-consuming and expensive. However, the asymptotic solutions (which require practically no computation) provide the best agreement with exact results in that very range. This feature must be exploited in industrial calculations whenever a low mass fraction situation is encountered.

The effect of laminar film condensation on the transport of a noncondensable but absorbable third component that is present in the mixture is illustrated in Fig. 9. Similar to the reference heat flux Q_{Nu} introduced in heat transfer descriptions, we introduce a standard reference mass flux, $\dot{m}_0$, in order to facilitate the mass transport discussion. This is derived from a pseudo-physical situation where a droplet is translating in a binary mixture of one component that has the same physical properties as steam but will not condense, while the other is a noncondensable but absorbable substance that exists in trace amounts. The flow field in this latter case is described by the Homann's solution [24]. Figure 9 corresponds to the ambient thermal condition of 125°C and a droplet size of 0.025 cm. It is clear that the convective inward motion at the interface (induced by the condensation) enhances the trace amount removal rate as compared to the reference case where there is no such interface velocity. As expected, with lower $w_{1,\infty}$, higher rates of third-component mass transfer are realized. For a given $w_{1,\infty}$, the dimensionless mass flux, $(\dot{m}/\dot{m}_0)$, initially experiences a rather steep increase with increasing ΔT, and with further increase of ΔT, it eventually levels off to an almost constant rate of removal as would be expected. Figure 9 also displays the effect of ambient thermal condition on third component removal. The ambient temperature is varied from 75 to 175°C. For given $w_{1,\infty}$, drop size, and ΔT, with increasing ambient temperature, the mass-transfer rate decreases. This same feature is observed with heat transfer.

SUMMARY AND CONCLUSIONS

Numerical solutions to the nonlinear, coupled boundary-layer equations governing laminar condensation heat and mass transfer in the vicinity of the stagnation point of a freely falling spherical droplet in a saturated mixture of three components are presented. The environment surrounding the droplet is composed of a condensable (steam), a noncondensable and nonabsorbable (air), and a third component which is noncondensable but absorbable (a typical fission product in a nuclear reactor containment following a loss of coolant accident). The flow field on the outside of the droplet is taken to be a

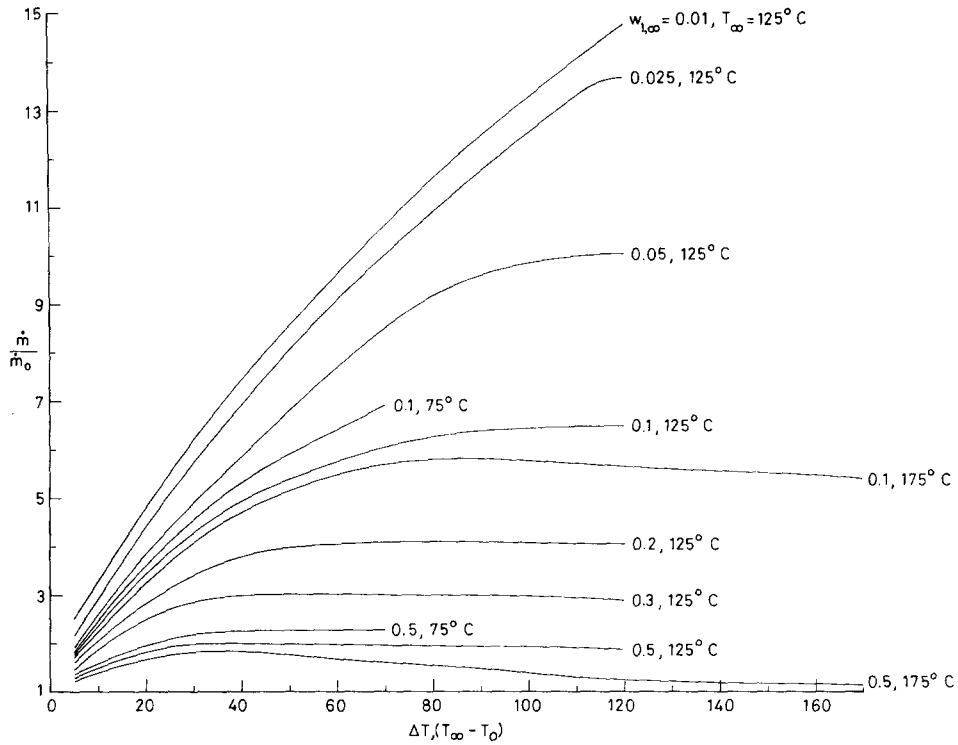

FIG. 9. Effects of $w_{1,\infty}$ and T_∞ on the absorption of the third component. $R = 0.025$ cm.

laminar boundary layer. The droplet also experiences a strong internal circulation. The results presented include cases that correspond to situations likely to be present in a nuclear reactor containment following a loss of coolant accident. The engineering value of this study is thus made apparent [26].

As would be expected, the presence of the noncondensables seriously inhibit the rate of heat and mass transfer. For a given thermal driving force and noncondensable gas concentration in the bulk, the dimensionless heat transfer decreases with increasing ambient saturation temperature. This is a novel feature observed in this study. It is also noticed that the weakening of the condensation flow field due to reduced terminal velocity of the droplet has a more serious effect on heat transfer than that of the increased ambient temperature (increased thermal driving force). For set thermal conditions, and noncondensable gas concentrations, the heat transfer is seen to increase with increasing droplet size.

The paper provides an asymptotic solution in the limit of vanishing noncondensable and nonabsorbable component. These solutions provide bounds and checks for the numerical results. It is noted that the asymptotic solutions agree very well with the numerical results even when the noncondensable gas concentrations are finite but small. In view of the simplicity of evaluating the final asymptotic solutions, they are recommended for convenient industrial use.

The paper also provides a study of the effect of laminar film condensation on the transport of a noncondensable but absorbable third component that is present in the mixture in trace amounts. The convective inward motion at the interface (induced by the condensation) enhances the trace amount removal rate as compared to the case where there is not such interface velocity.

An important conclusion stemming from the present study is that the droplet diameter, forced flow field velocity and the ambient thermodynamic conditions prevailing in the environment are all strongly influencing and mutually related factors that control the laminar condensation heat and mass transfer rates to a freely falling droplet. The dominant effect of the presence of a noncondensable gas does not require any further elaboration.

The presented results show good comparison with the existing limited experimental results appropriate to this work. From this investigation, it is apparent that, where large noncondensable gas concentrations and small thermal driving forces are encountered, the convective contribution (relative to the change of phase contribution to heat- and mass-transfer rates) may not be ignored if sufficiently accurate results are desired.

Acknowledgements—The authors wish to gratefully acknowledge the many helpful discussions they had with Professor A. M. Whitman (University of Pennsylvania), and Dr. S. D. Lin (United Engineers and Constructors, Inc., Philadelphia) during the course of this investigation. Sponsorship of this work by the National Science Foundation Grant ENG 77-23137 is also gratefully acknowledged.

REFERENCES

1. M. J. Boussinesq, Calcul du pouvoir refroidissant des courant fluids, *J. Math. Pures Appl.* **70,** 285 (1905).
2. R. Kronig and J. C. Brink, On the theory of extraction from falling droplets, *Appl. Scient. Res.* **A2,** 142–154 (1950).
3. W. Ranz and W. Marshall, Evaporation from drops, *Chem. Engng. Prog.* **48,** 141–146, 173–180 (1952).
4. B. T. Chao, Motion of spherical gas bubbles in a viscous liquid at large Reynolds numbers, *Physics Fluids* **5** (1), 69–70 (1962).
5. A. Acrivos and T. D. Taylor, Heat and mass transfer from single spheres in Stokes flow, *Physics Fluids* **5** (4), 387–394 (1962).
6. V. P. Vorotilin, V. S. Krylov and V. G. Levich, On the theory of extraction from a falling droplet, *J. Appl. Math. Mech.* **29** (2), 386–394 (1965).
7. V. G. Levich, V. S. Krylov and V. P. Vorotilin, On the theory of unsteady diffusion from moving drops, *Dokl. Akad. Nauk SSSR* **161,** 648 (1965).
8. A. Acrivos and J. Goddard, Asymptotic expansion for laminar forced convection heat and mass transfer, Part 1, *J. Fluid Mech.* **23** (2), 273–291 (1965).
9. S. Winnikow and B. T. Chao, Droplet motions in purified systems, *Physics Fluids* **9** (1), 50–61 (1966).
10. B. T. Chao, Transient heat and mass transfer to a translating droplet, *J. Heat Transfer* **91** (2), 273–281 (1969).
11. J. D. Ford and A. Lekic, Rate of growth of drops during condensation, *Int. J. Heat Mass Transfer* **16,** 61–64 (1973).
12. W. C. Strahle, Forced convection droplet evaporation with finite vaporization, kinetics and liquid heat transfer, *Int. J. Heat Mass Transfer* **15,** 2077–2089 (1972).
13. E. Ruckenstein, Mass transfer between a single drop and a continuous phase, *Int. J. Heat Mass Transfer* **10,** 1785–1792 (1967).
14. T. D. Sandry, Drop shapes and internal flow patterns by numerical solution of the Navier–Stokes equations, Doctoral Dissertation, Iowa State University (1973).
15. G. L. Hubbard, V. E. Denny, and A. F. Mills, Droplet evaporation: effects of transients and variable properties, *Int. J. Heat Mass Transfer* **18,** 1003–1008 (1975).
16. W. J. Minkowycz and E. M. Sparrow, Condensation heat transfer in the presence of non-condensables, interfacial resistance, superheating, variable properties and diffusion, *Int. J. Heat Mass Transfer* **9,** 1125–1144 (1966).
17. F. E. Sage and J. Estrin, Film condensation from a ternary mixture of vapors upon a vertical surface, *Int. J. Heat Mass Transfer* **19,** 323–333 (1976).
18. R. E. Bellman and R. E. Kalaba, *Quasilinearization and Non-Linear Boundary-Value Problems.* Elsevier, New York (1965).
19. H. Kutchai, J. A. Jacquez and F. J. Mather, Non-equilibriums facilitated oxygen transport in hemoglobin solution, *Biophysical Jl* **10** (1), 38–54 (1970).
20. A. Acrivos, Mass transfer in laminar boundary-layer flows with finite interfacial velocities, *A.I.Ch.E. Jl* **6** (3), 410–414 (1960).
21. R. K. Hillard, A. K. Postma, J. D. McCormack and L. F. Coleman, Removal of iodine and particles by sprays in the containment systems experiment, *Nucl. Technol., J. Am. Nuc. Soc.* **10,** 499–519 (1971).
22. C. E. Lapple, *Fluid and Particle Mechanics,* p. 284. University of Delaware, Delaware (1951).
23. V. E. Denny and V. South III, Effects of forced flow, noncondensables, and variable properties on film condensation of pure and binary vapors at the forward stagnation point of a horizontal cylinder, *Int. J. Heat Mass Transfer* **15,** 2133–2142 (1972).
24. F. Homann, Der Einfluß großer Zahigkeit bei der stromung um den Zylinder und um die Kugel, *Z. Angew. Math. Mech.* **16,** 153–164 (1936); and *Forsch. Geb. Ing-Wes.* **7,** 1–10 (1936).
25. J. W. Yang, Laminar film condensation on a sphere, *J. Heat Transfer,* **95** (2), 174–178 (1973).
26. J. N. Chung and P. S. Ayyaswamy, The Effect of internal circulation on the heat transfer of a nuclear reactor containment spray droplet, *Nucl. Technol., J. Am. Nuc. Soc.* **35** (3), 603–610 (1977).

APPENDIX A

Details of the asymptotic solution procedure

Consider the governing equations (50)–(53) and boundary conditions (54)–(55) of the text. Equation (50) with appropriate boundary conditions yields:

$$\phi(z) = z + \frac{Sc}{n}(e^{-(n/Sc)z} - 1). \tag{A1}$$

By substituting (A1) into equation (52) and solving subject to the appropriate boundary condition,

$$\psi'(z) = e^{-nz}\left\{1 - \frac{2Sc}{b^2}\left[\frac{z^2}{2} - \left(\frac{Sc}{n}\right)^2 \times (e^{-(n/Sc)z} - 1) - \frac{Sc}{n}z\right]\right\}, \tag{A2}$$

and

$$1 = \int_0^\infty e^{-nz}\left\{1 - \frac{2Sc}{b^2}\left[\frac{z^2}{2} - \left(\frac{Sc}{n}\right)^2 \times (e^{-(n/Sc)z} - 1) - \frac{Sc}{n}z\right]\right\}dz. \tag{A3}$$

The integral is evaluated to produce,

$$b = \left[\frac{2}{n^2(1-n)}\frac{Sc}{(1+Sc)}\right]^{1/2}. \tag{A4}$$

Substituting (A1) and (A2) into equation (53) and in the limit $b \to \infty$, with $\Theta_0 = \Theta(0)$,

$$\Theta'(z) = \Theta_0' \exp\left[-\int_0^z f(\bar{z})\,d\bar{z}\right] \tag{A5}$$

where

$$\int_0^z f(\bar{z})\,d\bar{z} = Pr_\infty\left[-\frac{\xi}{n}(e^{-nz} - 1) + \frac{n}{Sc}z\right], \tag{A6}$$

with

$$\xi = \frac{1}{Sc}\frac{C_{p_{1+2}}}{C_p}(w_{1,\infty} - w_{1,i}). \tag{A7}$$

Then,

$$(1 - \Theta_0) = \int_0^\infty \Theta_0' \exp\left\{-Pr_\infty\left[-\frac{\xi}{n}(e^{-nz} - 1) + \frac{n}{Sc}z\right]\right\}dz \tag{A8}$$

$$= \frac{\Theta_0'}{e^\alpha}\int_0^\infty \exp(A_1 e^{-nz} - A_2 z)\,dz. \tag{A9}$$

where,

$$\alpha = A_1 = Pr_\infty\frac{\xi}{Sc}, \quad A_2 = Pr_\infty\frac{n}{Sc}.$$

The integral in (A9) can be represented by an infinite series approximation as follows:

$$I = \int_0^\infty \exp(A_1 e^{-nz} - A_2 z)\,dz = \frac{1}{n}\sum_{j=0}^{\infty}\frac{A_1^j}{j!}\frac{1}{\left(\frac{A_2}{n} + j\right)}. \tag{A10}$$

Therefore,

$$\Theta_0' = \frac{(1-\Theta_0)\,e^{\alpha}}{I}. \tag{A11}$$

APPENDIX B

Nusselt's type of solution for pure steam condensing on a sphere

Consider an isothermal rigid sphere situated in a large body of quiescent pure vapor which is at its saturation temperature T_∞. The surface of the sphere is maintained at T_0 which is less than T_∞. A thin layer of condensate in the form of a continuous laminar film runs downward over the sphere. We shall assume that the temperature distribution in the condensate is linear. The thermodynamic properties for the liquid condensate are taken to be constants and the axial conduction in the film is neglected. Furthermore, the momentum changes in the liquid film, the shear forces at the vapor–liquid interface, and the thermal resistance at the interface are all neglected.

The governing equations then become:

$$\nu_l \frac{\partial^2 u}{\partial y^2} + \frac{g(\rho_l - \rho_v)}{\rho_l}\frac{x}{R} = 0, \tag{B1}$$

and

$$k_l \frac{\partial^2 T_l}{\partial y^2} = 0. \tag{B2}$$

The boundary conditions are:

$$\left.\begin{aligned} &T_l = T_0,\ u = 0,\ v = 0,\ \text{at } y = 0 \\ &T_l = T_\infty,\ \mu_l \frac{\partial u}{\partial y} = 0 \text{ at } y = \delta. \end{aligned}\right\} \tag{B3}$$

Introduce the similarity transformation parameters:

$$\left.\begin{aligned} &\eta = yC_*^{1/4}/R,\ C_* = g(\rho_l - \rho_v)R^3/\rho_l \nu^3, \\ &\Psi = \nu C_*^{1/4} x f(\eta)/R, \\ &u = \frac{1}{r}\frac{\partial}{\partial y}(\Psi r),\ v = -\frac{1}{r}\frac{\partial}{\partial x}(\Psi r), \\ &\Theta_l = (T_l - T_\infty)/(T_0 - T_\infty). \end{aligned}\right\} \tag{B4}$$

With these, the resulting ordinary differential equations are:

$$f''' + 1 = 0 \tag{B5}$$

and

$$\Theta_l'' = 0 \tag{B6}$$

subject to boundary conditions

$$\left.\begin{aligned} &f = 0,\ f' = 0,\ \Theta = 1 \text{ at } \eta = 0 \\ \text{and}\quad &f'' = 0,\ \Theta = 0 \text{ at } \eta = \eta_\delta. \end{aligned}\right\} \tag{B7}$$

A heat balance at the interface between vapor and liquid yields

$$-k_l \left.\frac{\partial T_l}{\partial y}\right|_{y=\delta} = \frac{\rho_l \lambda}{r}\frac{\mathrm{d}}{\mathrm{d}x}\int_0^\delta ur\,\mathrm{d}y \tag{B8}$$

where we have neglected the conduction heat flux from the vapor side.

With the transformation, the interface compatibility equation becomes

$$k_l(T_\infty - T_0)\Theta_l'(\eta_\delta) = 2\lambda\mu_l f(\eta_\delta). \tag{B9}$$

The analytical solutions to equations (B5) and (B6) can now be written down as

$$\left.\begin{aligned} f &= \frac{1}{6}\eta^3 - \frac{\eta_\delta}{2}\eta^2 \\ \Theta_l &= -(\eta/\eta_\delta) + 1. \end{aligned}\right\} \tag{B10}$$

Through the use of (B9),

$$\eta_\delta = \left[\frac{3}{2}\frac{k_l(T_\infty - T_0)}{\lambda\mu_l}\right]^{1/4}, \tag{B11}$$

and,

$$\delta = \left[\frac{3}{2}\frac{k_l\mu_l(T_\infty - T_0)R}{g(\rho_l)(\rho_l - \rho_v)\lambda}\right]^{1/4}. \tag{B12}$$

Next,

$$Q_{Nu} = h(T_\infty - T_0), \quad \text{and,} \quad h = k_l/\delta.$$

Therefore,

$$Q_{Nu} = \left[\frac{2/3\,k_l^3(T_\infty - T_0)^3 g\rho_l(\rho_l - \rho_v)\lambda}{\mu_l R}\right]^{1/4} \tag{B13}$$

and

$$Nu = \frac{hD}{k_l} = 1.075\left[\frac{g\rho_l(\rho_l - \rho_v)\lambda D^3}{k_l\mu_l(T_\infty - T_0)}\right]^{1/4}. \tag{B14}$$

Yang [25] has obtained a numerical solution to this same problem including the inertia effect. He presents the following correlation equation for the Nusselt number:

$$Nu = 1.098\left[\frac{g\rho_l(\rho_l - \rho_v)\lambda D^3}{k_l\mu_l(T_\infty - T_0)}\right]^{1/4}. \tag{B15}$$

We note that the effect due to inertia is indeed very small.

TRANSFERT DE CHALEUR ET DE MASSE EN CONDENSATION LAMINAIRE AU VOISINAGE DU POINT D'ARRET AMONT D'UNE GOUTTE SPHERIQUE EN TRANSLATION DANS UN MELANGE TERNAIRE: SOLUTIONS NUMERIQUE ET ASYMPTOTIQUE

Résumé—On présente des solutions numériques des équations non linéaires et couplées de couche limite représentant les transferts massique et thermique au voisinage du point d'arrêt amont sur une goutte sphérique en translation dans un mélange saturé de trois composants. Autour de la goutte, l'environnement est composé d'une vapeur condensable (eau) d'un gaz incondensable et non absorbable (air) et d'un troisième composant incondensable mais absorbable (un produit typique de fission dans un réacteur nucléaire par suite d'une perte accidentelle de réfrigérant). L'étude est faite dans les conditions suivantes: rayon de la goutte 0,005–0,05 cm, condition thermique ambiante 75–175°C, température initiale de la goutte 5–170°C et fraction massique du composant incondensable et non absorbable 0,01–0,5. Le troisième composant est sous forme de trace. On considère des solutions asymptotiques qui fournissent des limites et des contrôles pour les solutions numériques complètes. L'étude révèle plusieurs particularités. Un résultat nouveau est que, pour une concentration en gaz incondensable et un écart de température donnés, le transfert thermique adimensionnel décroît lorsque la température ambiante de saturation augmente. Une conclusion importante qui se dégage est que, pour une condensation laminaire en film sur une goutte tombant librement, la taille de la goutte, le champ des vitesses forcées et les

conditions thermodynamiques ambiantes sont tous des facteurs mutuellement reliés et déterminants qui contrôlent les flux de transfert. Les résultats présentés se comparent favorablement aux données expérimentales connues.

WÄRME- UND STOFFÜBERTRAGUNG BEI KONDENSATION IN DER NÄHE DES VORDEREN STAUPUNKTES EINES KUGELIGEN TROPFENS IN EINEM TERNÄREN GEMISCH

Zsammenfassung—Es werden numerische Lösungen der nichtlinearen gekoppelten Grenzschichtgleichung von Wärme- und Stoffübergang bei laminarer Kondensation in der Nähe des vorderen Staupunktes eines kugeligen Tropfens in einer gesättigten Mischung aus drei Komponenten angegeben. Das den Tropfen umgebende Fluid besteht aus einer kondensierbaren Komponente (Dampf), einer nicht kondensierbaren und nicht adsorbierbaren Komponente (Luft) und einer dritten Komponente, welche nicht kondensierbar, dafür aber absorbierbar ist, (ein typisches Spaltprodukt im Containment eines Kernreaktors nach einem Kühlmittelverlust-Unfall). Die Versuchsbedingungen umfaßten folgende Bereiche: Tropfenradien von 0,005–0,05 cm; Umgebungstemperaturen von 75–175°C; anfängliche Temperatur des Tropfens von 5–170°C; Massenanteile der nicht kondensierbaren und nicht adsorbierbaren Komponente, bezogen auf die Gesamtmasse, zwischen 0,01 und 0,5. Von der dritten Komponente wird angenommen, daß sie nur in Spuren vorhanden ist. Asymptotische Lösungen, die Grenzwerte und Kontrollen der vollständigen numerischen Lösung liefern, wurden ebenfalls bestimmt. Die Untersuchung zeigt einige interessante Merkmale. Ein neuer Gesichtspunkt ist der, daß bei einem gegebenen Temperaturgefälle und einem bestimmten Gasanteil im Gemisch die dimensionslose Wärmeübergangszahl mit zunehmender Sättigungstemperatur der Umgebung kleiner wird. Eine wichtige Schlußfolgerung ist, daß für laminare Film-Kondensation an einem frei fallenden Tropfen die Tropfengröße, die Geschwindigkeit und die äußeren thermodynamischen Bedingungen Faktoren von starkem wechselseitigen Einfluß auf den Wärmeübergang sind. Die erhaltenen Resultate zeigen gute Übereinstimmung mit den nicht sehr zahlreich vorliegenden experimentellen Ergebnissen.

ТЕПЛО- И МАССОПЕРЕНОС ПРИ ЛАМИНАРНОЙ КОНДЕНСАЦИИ ВБЛИЗИ ПЕРЕДНЕЙ КРИТИЧЕСКОЙ ТОЧКИ СФЕРИЧЕСКОЙ КАПЛИ, ПЕРЕМЕЩАЮЩЕЙСЯ В ТРЁХКОМПОНЕНТНОЙ СМЕСИ. ЧИСЛЕННОЕ И АСИМПТОТИЧЕСКОЕ РЕШЕНИЕ

Аннотация — Представлены численные расчёты системы нелинейных уравнений пограничного слоя, описывающих тепло- и массообмен при ламинарной конденсации вблизи передней критической точки сферической капли, перемещающейся в насыщенной трёхкомпонентной смеси, состоящей из конденсирующегося компонента (пар), неконденсирующегося и непоглощаемого компонента (воздух) и неконденсирующегося, но поглощаемого компонента (обычный продукт деления в противоаварийной оболочке ядерного реактора в случае аварии системы охлаждения). Радиус капли составлял от 0,005 см до 0,05 см, температура окружающей среды — от 75 до 175°C, начальная температура капли — от 5 до 170°C и массовая доля неконденсирующегося и непоглощаемого компонента — от 0,01 до 0,5. Предполагается, что третий компонент находится в смеси в незначительном количестве. Приведены также асимптотические решения, определяющие границы применимости и справедливость численных решений. Выявлен ряд интересных закономерностей, в том числе найдено, что при заданных перепаде температуры и концентрации неконденсирующегося газа в объёме безразмерный поток тепла уменьшается с увеличением температуры насыщения окружающей среды. В работе сделан важный вывод о том, что при ламинарной плёночной конденсации на свободно падающей капле такие факторы, как размер капли, поле скоростей вынужденного течения и термодинамические условия окружающей среды, зависят друг от друга и оказывают большое влияние на скорость переноса. Результаты расчётов хорошо согласуются с имеющимися в довольно ограниченном количестве экспериментальными данными.